Foreign Aid and Growth: A Sp P-VAR Analysis Using Satellite Sub-National Data for Uganda

Online Supplementary Material

Andrea Civelli
University of Arkansas

Andrew Horowitz
University of Arkansas

Arilton Teixeira
Ibmec

Abstract

This document provides additional material to the submitted version of the paper *Foreign Aid and Growth: A Sp P-VAR Analysis Using Satellite Sub-National Data for Uganda* for online publication.

S1 Sp P-VAR Specification and Diagnostic Assessment

This Section of the Appendix reports important details and results supplementing the discussion of the model selection in Section 4.1 of the paper.

S1.1 Spatial Autocorrelation

Table S1 illustrates the Moran's I global spatial autocorrelation index for *light* and *oda* along with the one-side p-value for statistical significance. One-side significance values are usually preferred in economic applications because the relevant case of spatial autocorrelation of economic variables is generally thought to imply positive correlations. The spatial autocorrelation is conducted for each year of the sample and it relies on the spatial contiguity matrix described in the main paper, which defines as neighbors two districts sharing a border. We find that the spatial autocorrelation of luminosity is consistently positive and significant across periods, while there is no indication of spatial autocorrelation for aid.[1]

Table S2 reports the Moran's I index for the estimated residuals of the baseline model. The spatial autocorrelation of the residuals of the luminosity equation is satisfactorily controlled for, while we observe more instances of spatial autocorrelation in the residuals of the ODA equation especially in the second most recent years of the sample.

[1]The index is computed using the Stata command *spatgsa*.

	Years																
	96	97	98	99	00	01	02	03	04	05	06	07	08	09	10	11	12
light	.276	.024	.199	.191	.191	.191	.234	.278	.256	.231	.142	.216	.227	.183	.229	.274	.325
	(.002)	(.005)	(.014)	(.017)	(.017)	(.017)	(.005)	(.001)	(.003)	(.006)	(.05)	(.008)	(.005)	(.02)	(.006)	(.002)	(.000)
oda	.201	0.079	.012	.041	-.037	.027	.087	.021	.032	-.135	-.089	-.004	.012	.041	.089	-.028	.002
	(.004)	(.104)	(.326)	(.238)	(.465)	(.268)	(.104)	(.296)	(.255)	(.146)	(.274)	(.396)	(.345)	(.043)	(.127)	(.496)	(.384)

Table S1: Moran's I spatial autocorrelation index for the two endogenous variables of the model. Spatial contiguity matrix define by shared borders. Sample 1996:2012, p-values in parentheses.

	Years												
	99	00	01	02	03	04	05	06	07	08	09	10	11
res_{light}	.219	.016	.076	-.029	-.132	.133	.122	-.119	.031	.357	-.088	.017	.288
	(.007)	(.335)	(.154)	(.238)	(.154)	(.061)	(.069)	(.187)	(.286)	(.000)	(.278)	(.328)	(.001)
res_{oda}	.162	.031	.287	.142	-.022	.200	.149	.206	.316	.213	.437	.094	.237
	(.029)	(.265)	(.001)	(.052)	(.316)	(.015)	(.036)	(.014)	(.001)	(.005)	(.000)	(.119)	(.005)

Table S2: Moran's I spatial autocorrelation index for the residuals of the baseline model. Spatial contiguity matrix define by shared borders. Estimation sample is 1996:2012, then the lags of the model and instruments, and the data transformation reduce the observed residual series to the years 1999:2011. P-values in parentheses.

S1.2 Cross Section Dependence and Time Autocorrelation

We conduct a Pesaran (2004)'s CD test on the same two sets of residuals as well. The tests strongly indicate cross-sectional dependence in both cases, with test statistics of 24.5 for the residuals of luminosity and 8.9 for the ODA residuals (both corresponding to p-values of zero). The average absolute values of cross section correlations are .33 and .30 respectively. Cross section dependence is then explicitly accounted for by transforming the data in deviations from the sample time averages (time demeaning).

The effectiveness of time fixed effects is assessed conducting the Sarafidis, Yamagata, and Robertson (2009)'s test on two dynamic panel data models that individually replicate each equation of the baseline Sp P-VAR. Although not exactly the same as the full VAR model, the equation-wise models try to exactly replicate the Sp P-VAR specification and estimation approach, and we believe these models offer a valuable guideline for our testing purposes. The dynamic panels are estimated by GMM using Roodman (2009)'s Stata package *xtabond2*. In particular, dynamic lags of both *oda* and *light* are used as the GMM *y*-instruments, while lags of the spatial terms and rainfall constitute the other instruments.[2] The results of these

[2]Instruments are automatically constructed by *xtabond2* replacing missing values with zeros, as suggested by Holtz-Eakin, Newey, and Rosen (1988), while this adjustment is not applied in our baseline regressions.

estimates are illustrated in the first two columns of Table S3.

Sarafidis, Yamagata, and Robertson (2009) show that time fixed effects (and time demeaning) are sufficient to eliminate the cross-section dependence in the residuals of a dynamic panel if the difference between the overall Hansen's J statistic and the statistic only for the non-y restrictions is not too large. The corresponding dynamic panel models of our baseline P-VAR (column a and b) satisfy this condition. We can take this as suggestive evidence that time demeaning in our P-VAR model is sufficiently mitigating concerns about cross-sectional dependence as well.

The same two columns of Table S3 provide information about the time serial correlation of the residuals of the models through the Arellano-Bond first-difference testing procedure. This test checks for autocorrelation in the first difference of the residuals. The first difference should always exhibit first-order autocorrelation since u_{t-1} is present both in Δu_t and Δu_{t-1}, but a second-order correlation in the difference is evidence of first-order autocorrelation in the level of residuals. As well known, the correctness of the choice of the lags of the y-instruments in the GMM estimation hinges on the lack of serial correlation. Column (b) illustrates that the residuals of the ODA equation have a first-order correlation (rejection of the null of no correlation at 1.1%). Further evidence about the first-order autocorrelation of the residuals is obtained from a P-VAR in the estimated residuals of a just identified P-VAR(1) model for *oda* and *light* in which only one-lag instrument is used. The estimates of the residuals VAR is reported in Table S4. The *oda* residuals exhibit a very significant autocorrelation and serial correlation with the *light* residuals too. Lagged *oda* residuals affect the current *light* residuals too.

We report in column (c) of Table S3 the estimates of the dynamic panel version of the *oda* equation of the P-VAR model that includes the fourth lag instrument then. As in columns (b) we find autocorrelation of the first order in the Arellano-Bond test, but we also find some autocorrelation of the fourth-order. This second result is quite important because, jointly with the response functions in Figure S1, it suggests to limit the range of lagged y-instruments to 2 and 3 only. The Hansen's J statistic is only marginally significant, but more importantly the difference-statistic for the y instruments (excluding the other instruments) clearly rejects (with p-value .03) the exogeneity of these instruments.

Finally, as a last piece of evidence about this high-order autocorrelation in the residuals, we compare the time-space response of the just identified Sp P-VAR in Figure S1, which we can say with confidence does not satisfy exogeneity of the GMM restrictions, with the response from an Sp P-VAR model that uses lags 2 to 4 as y-instruments. In both cases the response of nightlights to the ODA shock becomes negative on impact, and the response reverts to zero after that. This response is largely at odds with that in the baseline model.

We conclude this Section with the histogram of the estimated residuals of the baseline P-VAR model, along with a QQ plot for normality distribution visual assessment, and the plots of the ODA and light series by district. Figures S2 and S3 illustrate the histograms and QQ plots respectively. Overall, the distributions are normal, but with some heave tails in both residuals, on the left for lights and on the right for oda. However, since the GMM does not rely on normality of the residuals, this is a relatively secondary concern.

	$light_{i,t}$ (a)	$oda_{i,t}$ (b)	$oda_{i,t}$ (c)
$light_{i,t-1}$	.709	.008	-.018
	(.127)***	(.091)	(.126)
$oda_{i,t-1}$	.043	.658	.671
	(.066)	(.069)***	(.093)***
$rain_{i,t}$	.230	-5.871	.29
	(1.995)	(2.623)**	(2.896)
$\overline{lights}_{i,t}$	.015	.833	.305
	(.234)	(.267)***	(.236)
$\overline{oda}_{i,t}$	-.038	-.411	-.046
	(.156)	(.224)*	(.228)
N. of Obsservations	504	504	468
N. of Instruments	10	10	14
Arrelano-Bond Tests - First Difference			
For AR(1)	z=-3.37	z=-4.56	z=-3.78
	[.001]	[.000]	[.000]
For AR(2)	z = .21	z=-2.55	z=-.23
	[.835]	[.011]	[.818]
For AR(3)	z = -.02	z=1.29	z=.86
	[.987]	[.197]	[.392]
For AR(4)	z = -.13	z=.46	z=-1.09
	[.895]	[.647]	[.275]
For AR(5)	z = .23	z=1.22	z=2.24
	[.818]	[.224]	[.025]
Difference in Hansen Tests			
All IV	$\chi^2(5) = 7.20$	$\chi^2(5) = 2.52$	$\chi^2(9) = 16.50$
	[.206]	[.774]	[.057]
Excluding Y-IV	$\chi^2(1) = .52$	$\chi^2(1) = 1.02$	$\chi^2(3) = 3.21$
	[.469]	[.313]	[.360]
Difference	$\chi^2(4) = 6.67$	$\chi^2(4) = 1.50$	$\chi^2(6) = 13.29$
	[.154]	[.827]	[.039]

Table S3: Dynamic panel estimation of the single P-VAR equations – Columns (a) and (b) replicate the baseline specification; column (c) uses lags 2 to 4 as instruments. S.E. in parenthesis; p-values in brackets; significance levels 1%, 5%, and 10% indicated by *** , ** , and *.

	$light\ res_t$ (a)	$oda\ res_t$ (b)
$rlight\ res_{t-1}$	.019	.084
	(.061)	(.043)**
$oda\ res_{t-1}$	-.087	.198
	(.046)*	(.967)**
F.E.	Y	
Obs.	468	
N. of Panels	36	
Instruments	$L1$	

Table S4: P-VAR in the residuals estimated from a just identified version of the main paper model. Standard errors indicated in parenthesis, with significance levels of respectively 1%, 5%, and 10% indicated by *** , ** , and *.

(a) Only first lag instrumentation

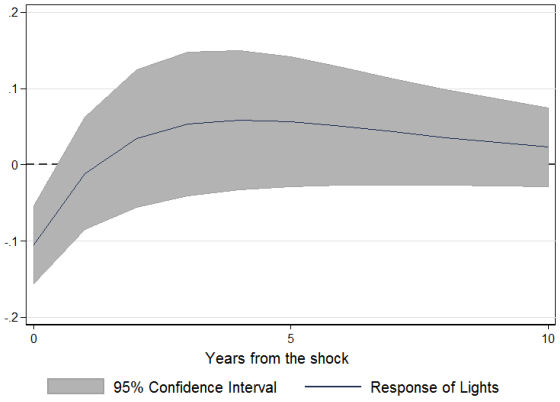

(b) Lags 2 to 4 instrumentation

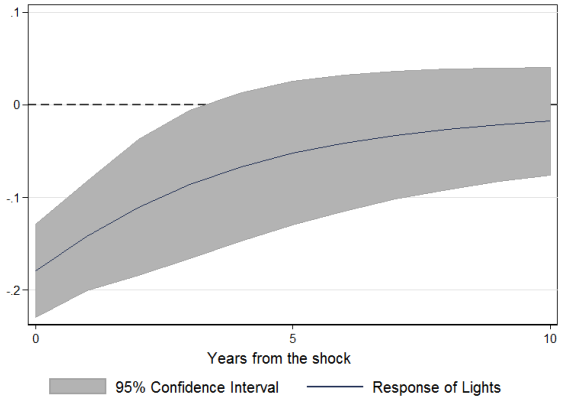

Figure S1: Sp P-VAR specification assessment – Time-space responses of nightlights to a one standard deviation shock to ODA. Years from the shock on the x-axis.

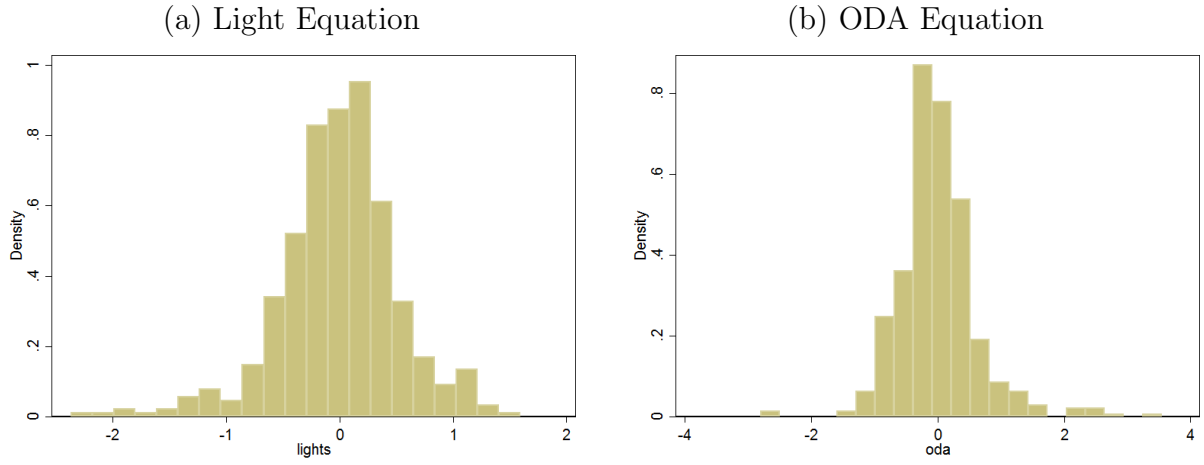

Figure S2: Sp P-VAR model: Histogram of the estimated residuals of the baseline model.

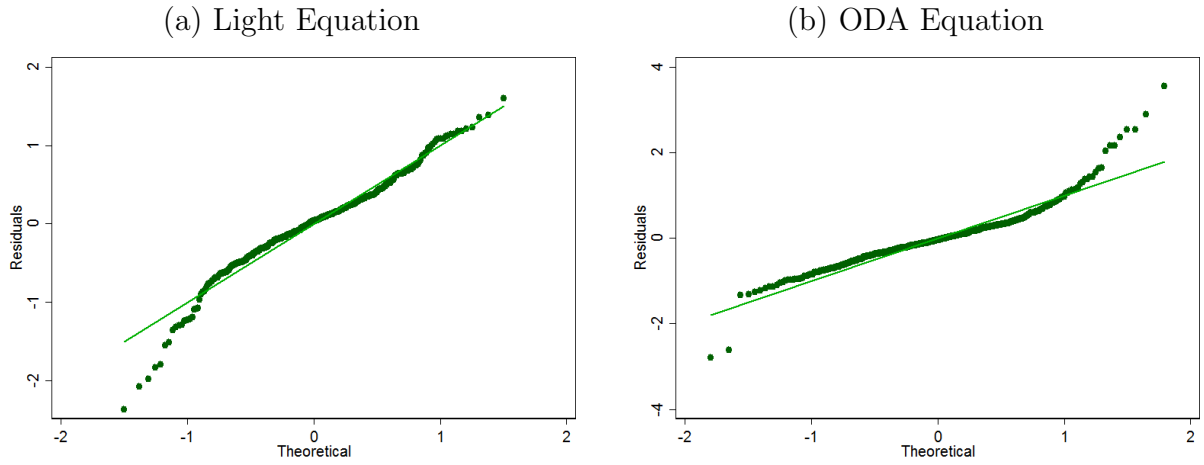

Figure S3: Baseline Sp P-VAR: QQ plots for the normality distribution of the residuals.

S1.3 Panel Unit Root Tests

Figures S4 and S5 illustrate the time series of the two endogenous variables of the model from which the cross-section mean has been subtracted for each point in time. We report in Tables S5 and S6 the results of the panel unit root tests used to support the Arellano-Bond GMM estimation approach of the Sp P-VAR in the paper.

When testing for panel unit roots in a panel framework, two types of tests are available depending on whether cross-sectional dependence is explicitly taking into account by the test procedure. The so called first generation tests are based on the cross-sectional independence assumption. Different options are available for this type of test, but probably the most established test of this group is the IPS test by Im, Pesaran, and Shin (2003). This test does not account for cross-sectional dependence, but allows for heterogeneity in the presence of unit root across panels and it is based on individual (augmented) Dickey-Fuller (ADF) statistics averaged across groups. The null of a unit root for all the series of the panel is contrasted to the alternative hypothesis that some (but not all) of the individual series to have unit roots.

In order to check to what extent this test could apply to our variables, we conduct a preliminary Pesaran (2004)'s CD test on the the two endogenous variables of the model for generic cross-section independence. In spite of the specific form of spatial correlation found in the data, the CD tests strongly indicate the cross-sectional independence null is not rejected for both variables, with test statistics of .93 for ODA and $-.86$ for nightlights (p-values of .35 and .39 respectively). This evidence, and the discussion in Section 4.1 of the paper, allows us to gather some initial evidence about the stationarity of aid and nightlight from the IPS test. Table S5 illustrates the results for this test, in which the ADF equations are specified with a constant (drift), but no time trend.[3] The IPS statistics are largely negative for all specifications, rejecting the null hypothesis of non-stationarity at more than 1% significance level with either AIC and BIC used as selection criteria for the lags in the ADF equation.

The second generation tests relax the cross-sectional independence assumption. The issue of how to specify the cross-sectional dependence is not obvious and different solutions are possible. We consider two related tests in which the cross-sectional dependencies are modeled as common factors by decomposing the individual series of the panel into three components: a deterministic component, a common component, and an idiosyncratic error term. This type of approach has been introduced by Bai and Ng (2004), who developed the popular PANIC Test in which the common component is estimated by using principal components. A variation of this test is PANICCA by Reese and Westerlund (2016), where principal components in the PANIC approach are replaced with cross-section averages.

These tests test for stationarity of the common and idiosyncratic components separately, and overall stationarity of the series is achieved if both of the components are stationary. Bai and Ng (2004) develop a set of different statistics to test for stationarity in the two components (MQ_c and MQ_c for multiple factors; P_a, P_b, and $PMSB$ for the idiosyncratic term in Table S6). An ADF statistics is used by PANICCA since only one common factor is used. These statistics are reviewed in Reese and Westerlund (2016).

Table S6 illustrates the results for these tests, in which the deterministic component

[3]Since all the tests presented here reject the non-stationarity of the variables of the model already with a basic drift specification, the time trend is excluded.

of the series is a specified with a constant (drift) again. The values of the statistics are typically negative and strongly significance for both *oda* and *light* for different specifications of the PANIC test as well as for PANICCA; the results do not depend on the use of AIC or BIC as selection criteria for the lags in the ADF equation; the significance of the tests is consistently higher than 5%, but it slightly deteriorates settling at about 10% for *oda* when a larger number of common factors is selected. Overall the results in these two tables allow us to assume stationarity of the endogenous vector with confidence.

IPS Test				
	light		*oda*	
Stat.	-7.74	-7.79	-2.77	-2.77
	(.000)	(.000)	(.003)	(.003)
N	36	36	36	36
T	17	17	17	17
Lag Criteria	AIC	BIC	AIC	BIC

Table S5: IPS Panel unit root tests for *oda* and *light*. IPS test by Im, Pesaran, and Shin (2003) and implemented in Stata with *xtunitroot, ips* command. Variables are cross-section demeaned. Statistics p-values reported in parentheses. The null hypothesis is non-stationarity.

	PANIC Test				PANICCA Test	
	light		*oda*		*light*	*oda*
ADF					-3.98	-3.86
					(.000)	(.000)
MQ_c	-16.65	-15.26	-15.98	-16.78		
	(.000)	(.000)	(.000)	(.000)		
MQ_f	-10.37	-14.50	-8.87	-15.06		
	(.000)	(.000)	(.000)	(.000)		
P_a	-7.47	-4.53	-3.72	-1.54	-8.98	-5.32
	(.000)	(.000)	(.000)	(.062)	(.000)	(.000)
P_b	-4.21	-3.04	-2.49	-1.25	-4.48	-3.08
	(.000)	(.001)	(.006)	(.105)	(.000)	(.001)
PMSB	-2.39	-1.98	-1.89	-1.09	-2.26	-2.22
	(.008)	(.024)	(.029)	(.138)	(.012)	(.013)
N	36	36	36	36	36	36
T	17	17	17	17	17	17
Lag Criteria	BIC	BIC	BIC	BIC	AIC	AIC
N. Factors	3	5	3	5	1	1

Table S6: PANIC and PANICCA Panel unit root tests for *oda* and *light*. PANIC test by Bai and Ng (2004) and PANICCA test by Reese and Westerlund (2016); implemented in Stata using the *xtpanicca* package. Variables are cross-section demeaned. Statistics p-values reported in parentheses. The null hypotheses are non-stationarity for the the common and idiosyncratic components. See Reese and Westerlund (2016) for the definition of the statistics.

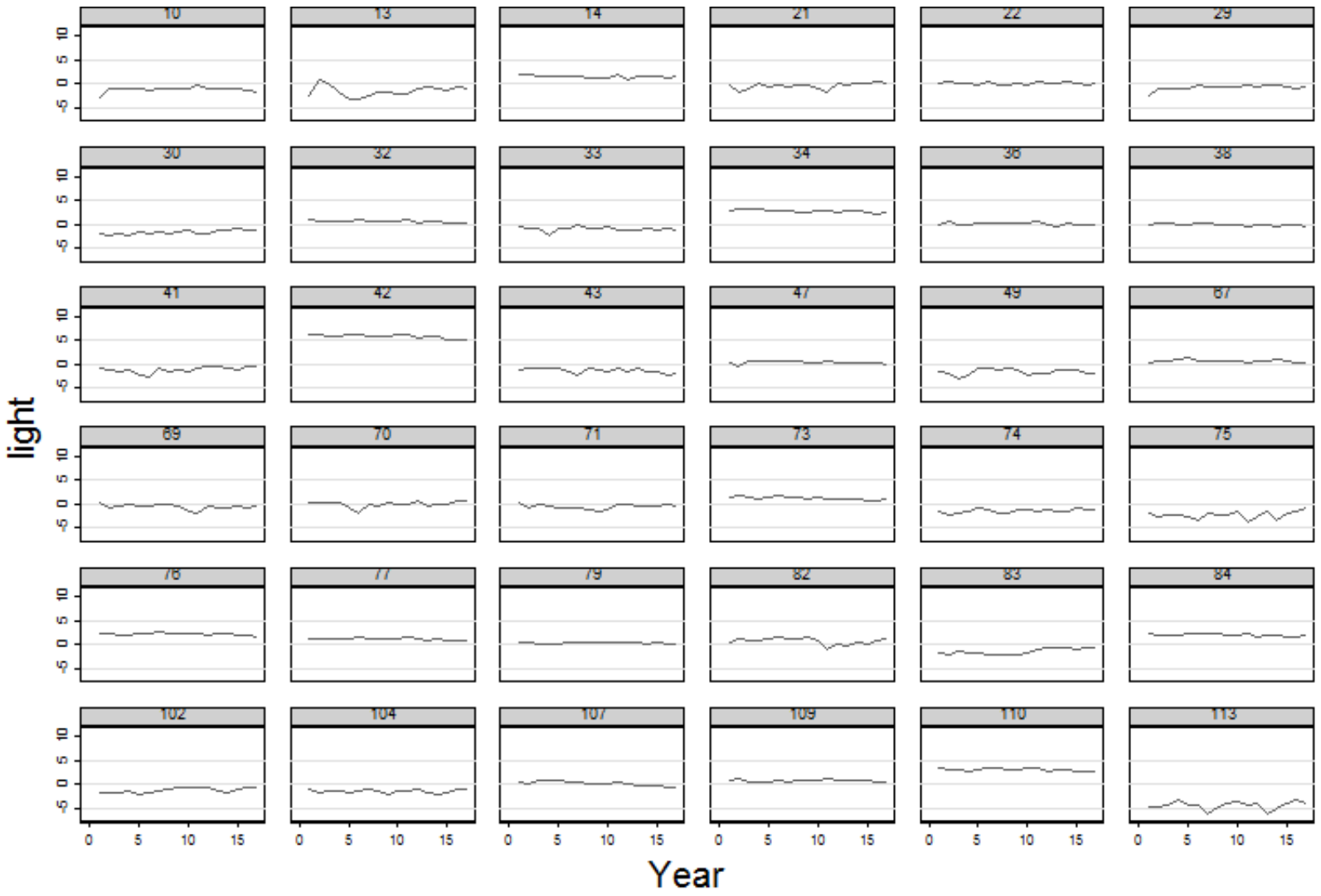

Figure S4: Time series of the variable $light_{i,t}$ by district in deviation from cross-section means.

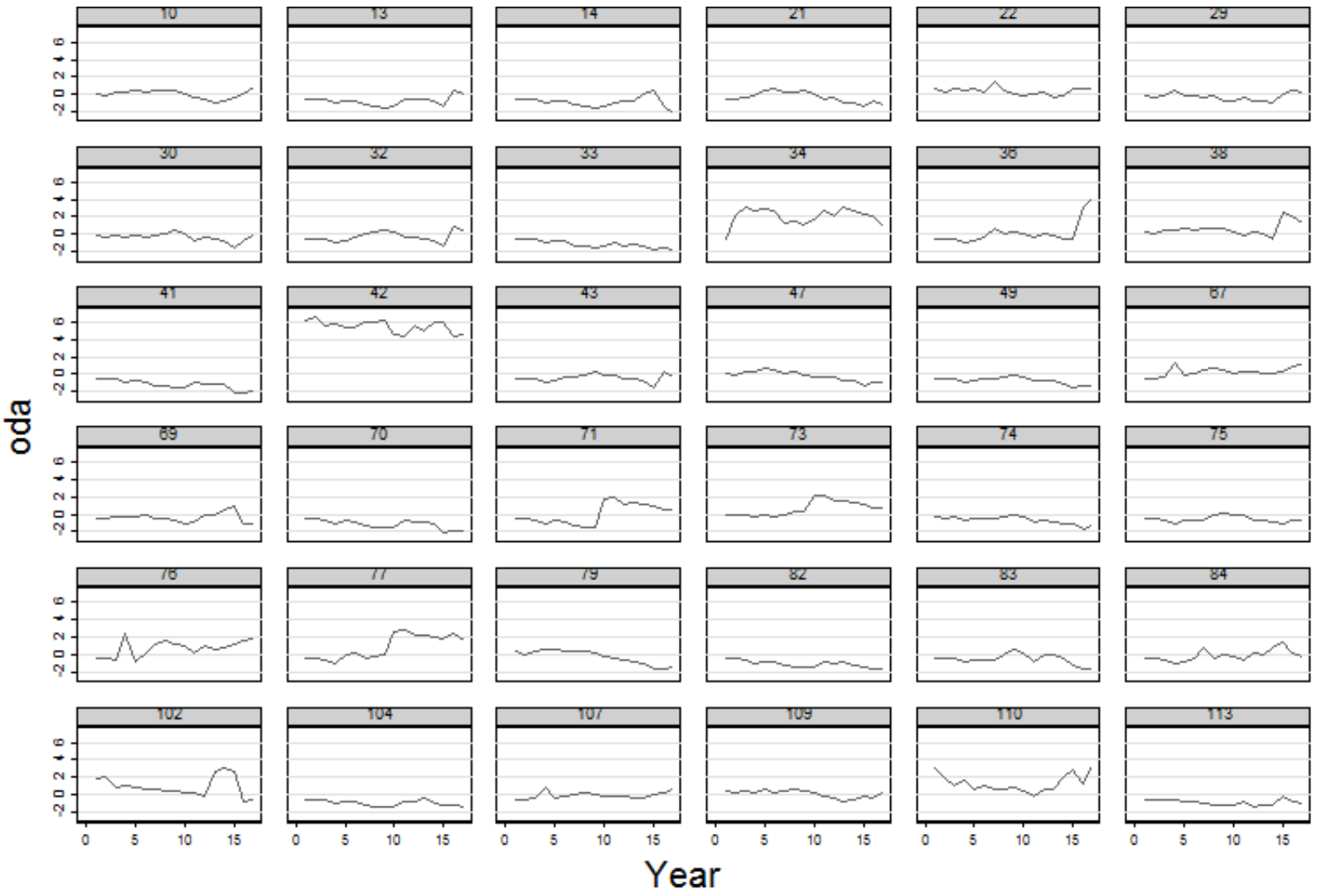

Figure S5: Time series of the variable $oda_{i,t}$ by district in deviation from cross-section means.

S2 Predictive Model Diagnostic Assessment

The predictive model is a panel with $T = 2$ only, which is then estimated with fixed effects in differences. Given the most basic form of panel when the time observations are only 2, autocorrelation and cross-sectional dependence of the residuals are a relatively secondary issue to consider since there is no time dimension on which test these correlations. Nevertheless, we can at least check for the specific type of cross section dependence due to spatial autocorrelation, which we explicitly account for in the regression model by spatially filtering the data before estimation. Table S7 illustrates the degree of spatial autocorrelation measured by the Moran's I index of the variables used in the two versions of the predictive model (equation 3 in the paper) we estimate. The Eigenvalues spatial filtering technique gently separate the spatial component of a spatial variable from the "trend" component; we see that post-filtering autocorrelations significantly drop. As a consequence, the residuals of the regressions should exhibit only small spatial autocorrelation. For the model with household weekly consumption expenditure the Moran's I is still somewhat large and significant (.161 with p-value .04), while for the model with average household monthly expenditure in non-durable goods the index is .124 (p-value .07).

We test for heteroskedasticity in the residuals of the two panel models sing the modified Wald statistic for group-wise heteroskedasticity in the residuals of a fixed effect regression model. In both cases the test strongly reject homoskedasticity (p-values of 0), therefore we proceed with a correction for heteroskedasticity-robust standard errors in the regression. Finally, we use a series of plots to assess the normality of the residuals (Figure S6) and to investigate for the presence of outliers in the data (Figure S7) for the two versions of the model.

For the normality, we use a standard QQ plot of the residuals Vs. a normal distribution. We do not observe large deviations from the normality distribution or systematic patterns in the residuals. For the outliers, we use a scatter plot of expenditure variable Vs. the nightlight variable. The paper describes the differences in definition of the expenditure variable for either version of the model. Also in this case, we don't find observations that particularly emerge as outliers.

	Original		Filtered	
	99	09	99	09
weekly expendit.	-.114	.319	.073	.135
	(.194)	(.000)	(.167)	(.059)
monthly expendit.	.144	.260	.055	.066
	(.047)	(.003)	(.210)	(.186)
light	.211	.259	.107	.102
	(.010)	(.002)	(.097)	(.103)

Table S7: Moran's I spatial autocorrelation index for the expenditure variables and luminosity used in the predictive regression (3) of the paper. Spatial contiguity matrix define by shared borders. P-values in parentheses.

(a) Weekly Expenditure

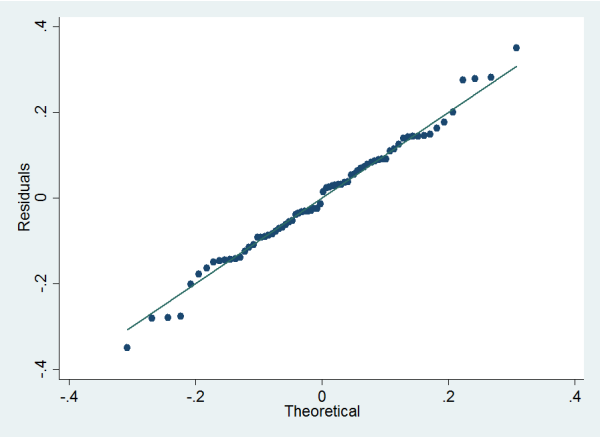

(b) Monthly Expenditure

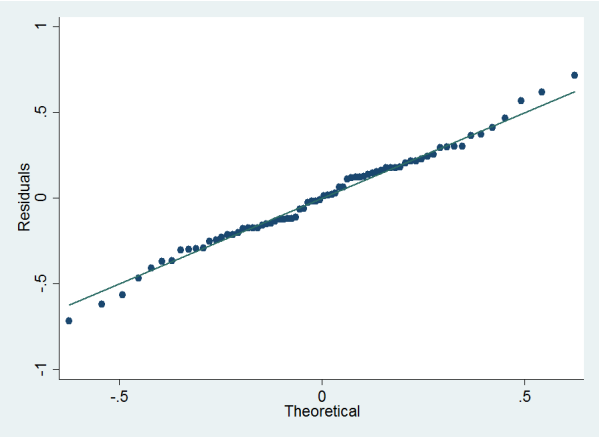

Figure S6: Predictive model - equation (9) in the main paper: QQ plots for normality distribution of the residuals.

(a) Weekly Expenditure

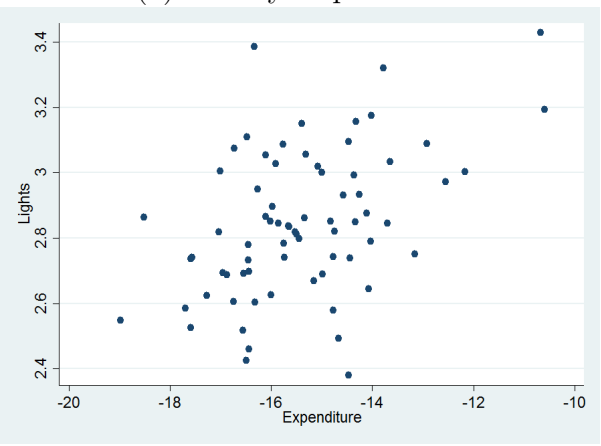

(b) Monthly Expenditure

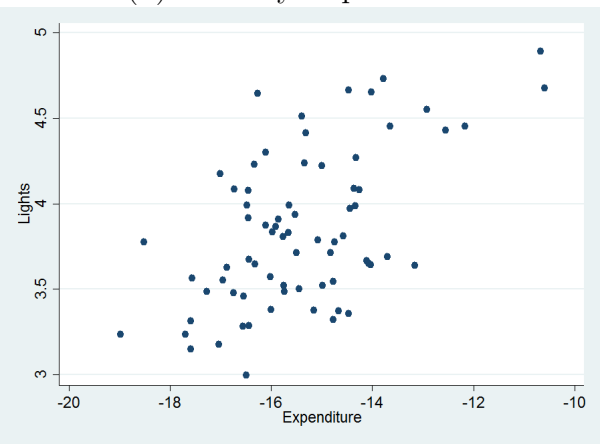

Figure S7: Predictive model - equation (9) in the main paper: scatter plots of expenditure Vs. nightlights.

S3 Results Robustness Assessment

Following the discussion of the robustness checks in Section 4.2 of the paper, this Section illustrates the results for the additional robustness exercises as mentioned in the main paper.

S3.1 Extended Robustness Checks

We start with Figures S8-S13, in which we drop one district at the time and recompute the time-only impulse response functions under the same baseline specification. As an important detail we note that, while a district is excluded from the cross-section of the panel, it is kept in the definition of the spatial contiguity matrix and the spatial terms. Overall, we find only small differences across district samples, with one important exception represented by District 42 which corresponds to the Kampala District – the capital district. Without this district, the response is still positive on impact but it drops in magnitude and significance very rapidly. Kampala gives an important contribution to the persistence of the response because it is the largest and more modern business and economic hub of the country. We discuss a similar case in robustness (e) of the paper, which is also the first case of Figure S14.

In Figures S14-S15 we propose a similar exercise in which we check how the responses change when we exclude small subsets of neighbor districts (ranging from two to four). The first of these cases is used for robustness (e) in the paper and discussed there. We analyze ten representative clusters: besides the Kampala metropolitan region, we consider the cluster on the West, North and East of that region, subsets of districts on the lake Victoria shore (notably Jinja, the other large metro area, is Subset 9), one cluster in the far North, one on the border with Rwanda (South), with Kenya (East), and with Congo (West). All these figures together satisfactorily confirm the stability of the time-only impulse response functions to sample variations.

We report next the time-only impulse response function of the P-VAR model under the alternative identification ordering of the structural shocks in Figures S16-S17. As discussed in Section 4.2, this identification produces different responses to both ODA and light shocks. In particular, luminosity does not respond to oda at all, whereas oda respond positively to light shocks. This type of response posits some serious interpretative difficulty of the estimated effects.

Finally, we consider the specification of the model that only uses the second-lag of Y as an instrument. Figure S18 reports the time-space response for this case. The initial part of the response is smaller than in the baseline and hump-shaped; on the contrary, the responses are closely comparable in magnitude in the medium and long-run. Although never statistically significant, the mean response is always positive; and, importantly, the long-run effects of aid on nightlight are preserved. As known, the precision of the GMM estimation can worsen with fewer instruments. This is what happens in this case too, as reflected by the slightly larger confidence intervals in the figure, which further lowers the significance of the IRF.

S3.2 Additional Exercises and Results

We provide first a short comment on the World Bank data base that we explored as an alternative to the AidData ODA disbursement. Figure S20 illustrates the time series of ODA by district, which can be compared to the one we use in Figure S5. The behavior of the World Bank disbursements noticeably differs from our dataset and this can have interesting insights for our analysis. The number of "zero" observations is also much higher than in the AidData dataset though. The zeros are about 75% (they are 20% in our case), and the World Bank does not make any donation to Uganda in 2011 and 2012 either. Keeping in mind that the estimation of a panel VAR model requires balanced panel structures ans suitable time series observations across units, the effect of this large share of zero observations is reflected by the size of the ODA shock Figure S19, which has a standard deviation more than 4 times bigger than in our baseline Sp P-VAR, and in the smaller response on impact of nightlights. However, the mean response of nightlight is positive and quite persistent, and the long-run effect of ODA shocks is preserved with this dataset as well. The 2-year elasticity, for instance, is 12%, which is closely comparable to the 16% of the main model.

The second exercise in this section explores the differences between early-impact and late-impact ODA disbursements. This exercise studies 22 districts of the 36 used in the main analysis, which receive more than just a couple of early-impact disbursements over the time sample 1996-2012. Figure S22 illustrates the time series of the early-impact ODA by district, which can be compared to the one we use in Figure S5. An important characteristic of early-impact aid in the AidData dataset is that this type of ODA seems to become more common in the second part of the sample; also for the other districts that receive only a small number of early-impact disbursements (and are not included in the 22 of this analysis), early-impact aid usually occurs in the last five years of the sample.

Figure S21 decomposes the time-only response of lights to an overall ODA shock into a component due to early-impact ODA and the remaining portion that can be attributed to late-impact aid.[4] The top panel of the figure shows the overall response: the impact response is positive, but the persistence of the IRF is weaker than in the baseline case. If the identification strategy adopted in the VAR model is plausible, the within-year and the short-term positive responses of nightlights to ODA should mainly come in response to shocks to early-impact aid, while late-impact aid shocks should be responsible for the long-term dynamics of the responses. Figure S21 provides evidence strongly consistent with this interpretation of the underlying mechanism of the identification strategy.

We find two important differences between the two components of the response. First, the middle panel illustrates the response of lights to an early-impact ODA shock. The short-term increase in lights is completely caused by the early-impact response. The effects of this type of aid are not very persistent, and they even turn negative in the medium-run. Second, the bottom panel shows the difference between overall and early-impact responses; this residual conceptually corresponds to the response to late-impact ODA. Late-impact aid has a smaller effect at the beginning of the response, but it then gain strength in the medium to long-run between 5 and 10 years since the shock. It actually compensates the negative portion of the early-impact response, summing up to a null overall effect. The effects of

[4] An analogous decomposition would be obtained with time-space IRF, we focus then on the simplest direct case.

late-impact ODA are always positive and also very persistent.

We conclude this Appendix with some output that indirectly justifies the importance of using the spatial features of the model. The first in Figure S23 is the IRF of a simple P-VAR model estimated without any spatial component. In this model, not only the responses to an ODA shock mix time and space dimension of the transmission mechanism, but they also are obtained from biased estimates in which the endogenous spatial terms are not correctly controlled for. On the left side panel, we consider a specification without time fixed effects. The IRF are positive and significant, not too different in magnitude from our baseline result. The specification of the model on right side panel includes time effects too; the IRF are still positive, but smaller and not significant anymore. The use of time effects, which captures cross-sectional factors, absorbs most of the dynamics of the IRF in the non-spatial model. These figures are a good comparison point for our results, because the introduction of spatial features in the model are expected to correct the dynamics of the model, without however introducing fundamental shifts.

The last observation is based on Figure S25, where the impulse response of lights to an ODA shock is computed from a model in which only one third (i.e. 12) of the 36 districts of the main analysis are sampled in such a way that no borders are shared anymore. A P-VAR is then estimated under the standard specification of the model including the time effects. These "isolated" districts form a map in which spatial spillovers are strongly weakened and the transmission of the shocks across neighbors should be muted. Figure S24 shows the districts included in this example. The spatial VAR we estimate is meant to capture the spatial spillovers across units, and we would expect similar effects in the two models. Figure S25 illustrates how shape, magnitude, and significance of the IRF are maintained in the aspatial model too. A caveat about this last result is that, clearly, multiple maps can be obtained drawing some non-spatially connected districts from the original set. We experiment with a few combinations and the results seem fairly stable, even though it is possible to find cases in which the response is not significant or negative.

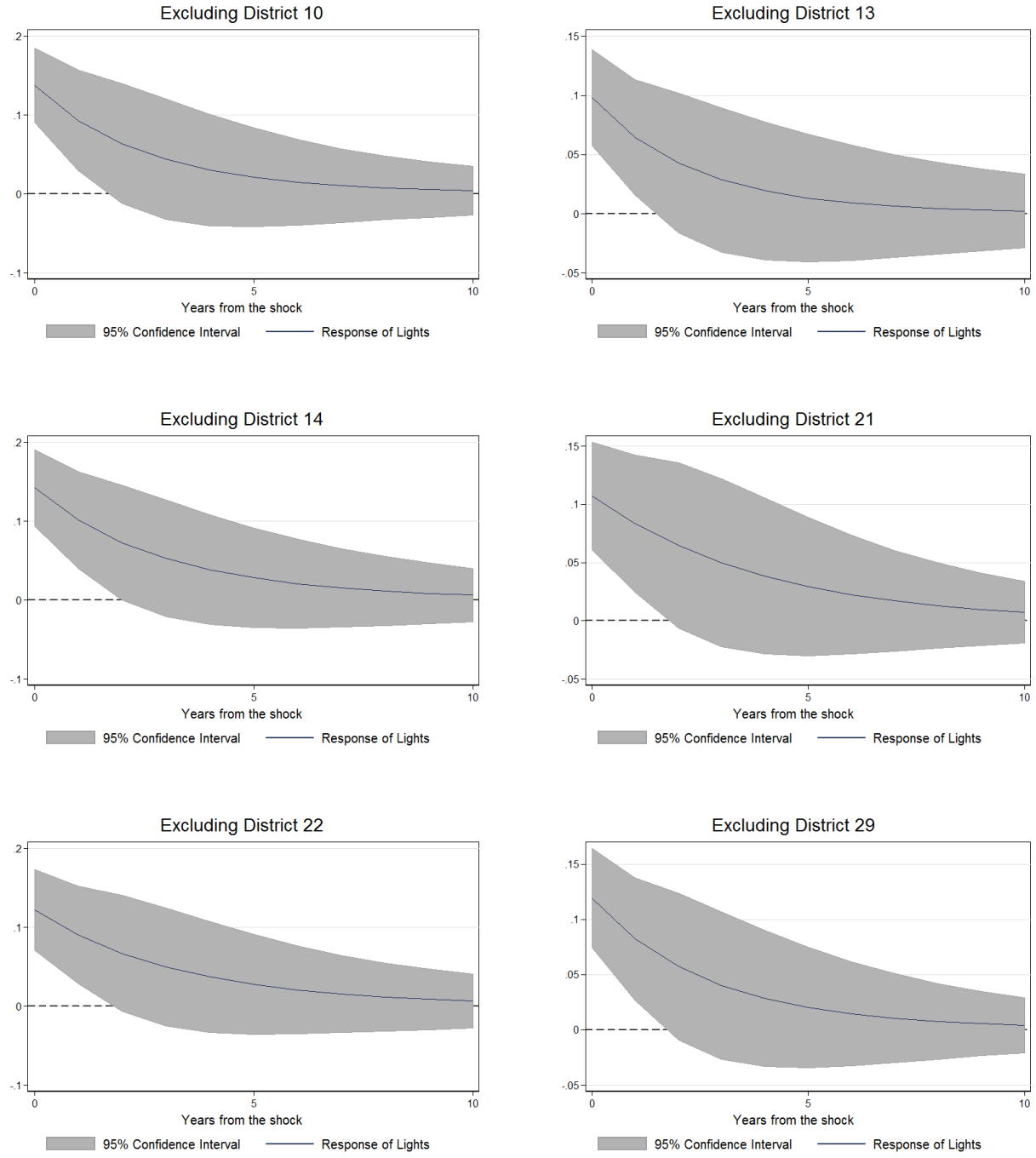

Figure S8: EXCLUDING DISTRICTS 1 – Time-only responses of nightlights to a one standard deviation shock to ODA excluding one district at the time. Years from the shock on the x-axis.

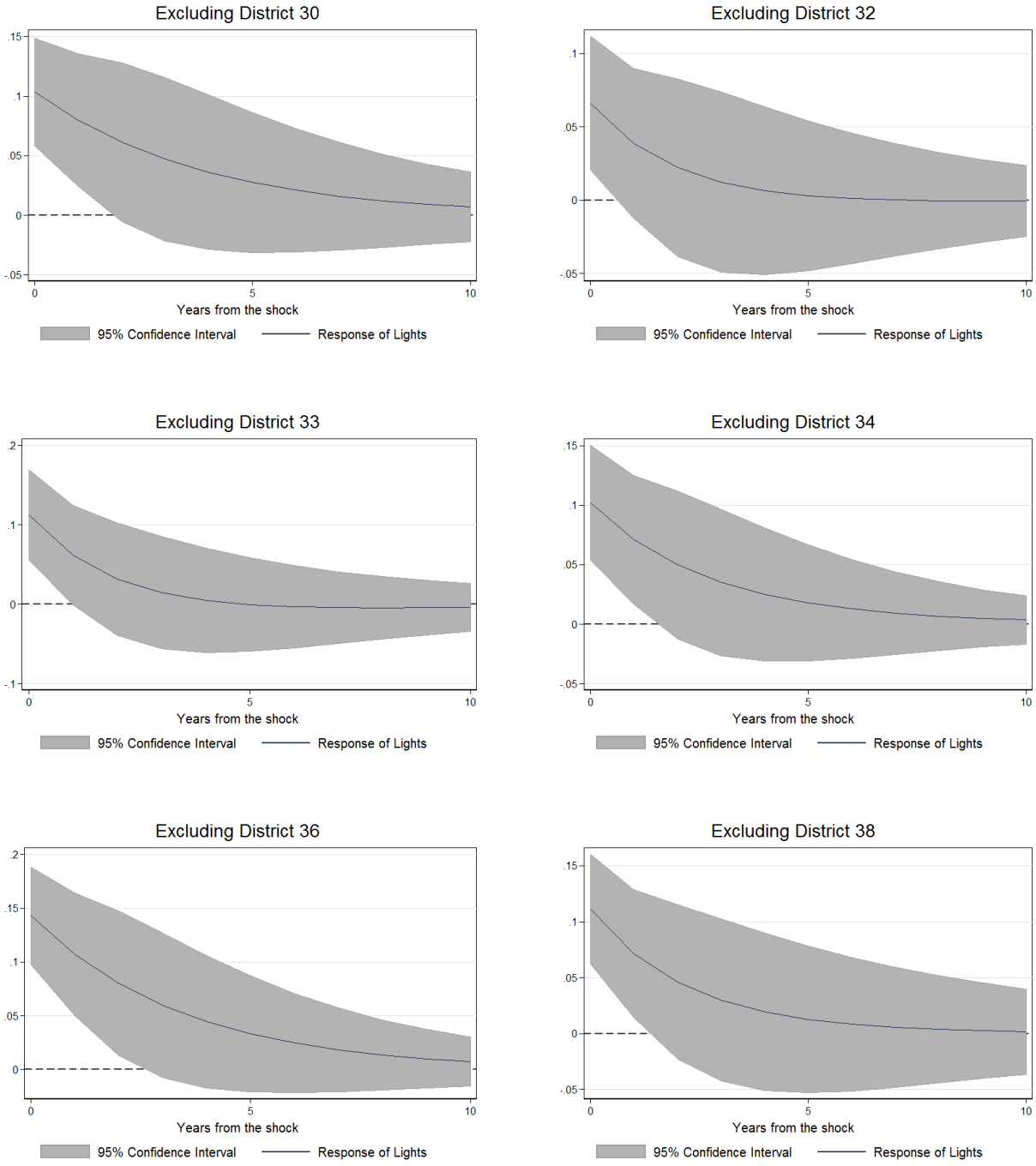

Figure S9: EXCLUDING DISTRICTS 2 – Time-only responses of nightlights to a one standard deviation shock to ODA excluding one district at the time. Years from the shock on the x-axis.

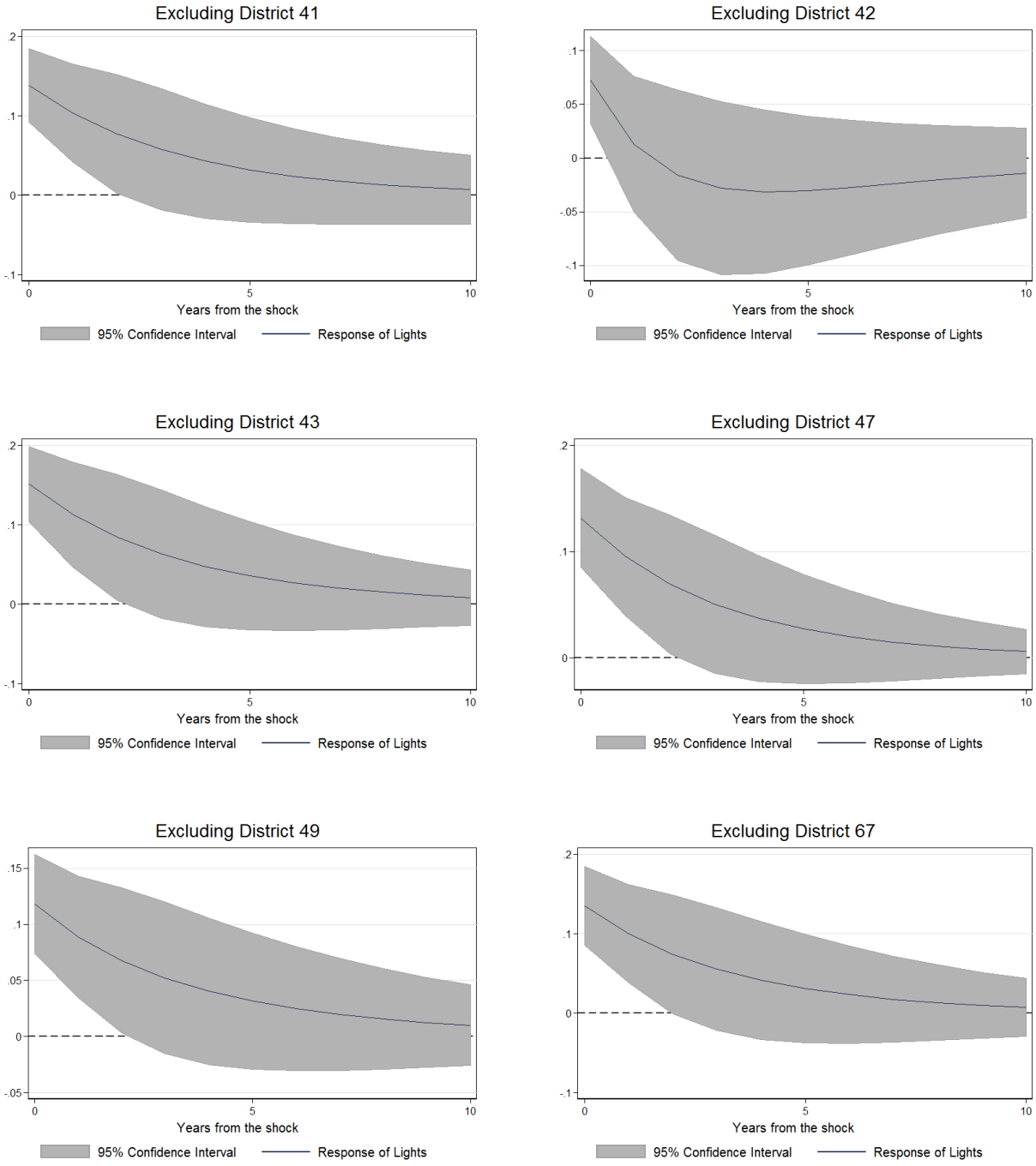

Figure S10: EXCLUDING DISTRICTS 3 – Time-only responses of nightlights to a one standard deviation shock to ODA excluding one district at the time. Years from the shock on the x-axis.

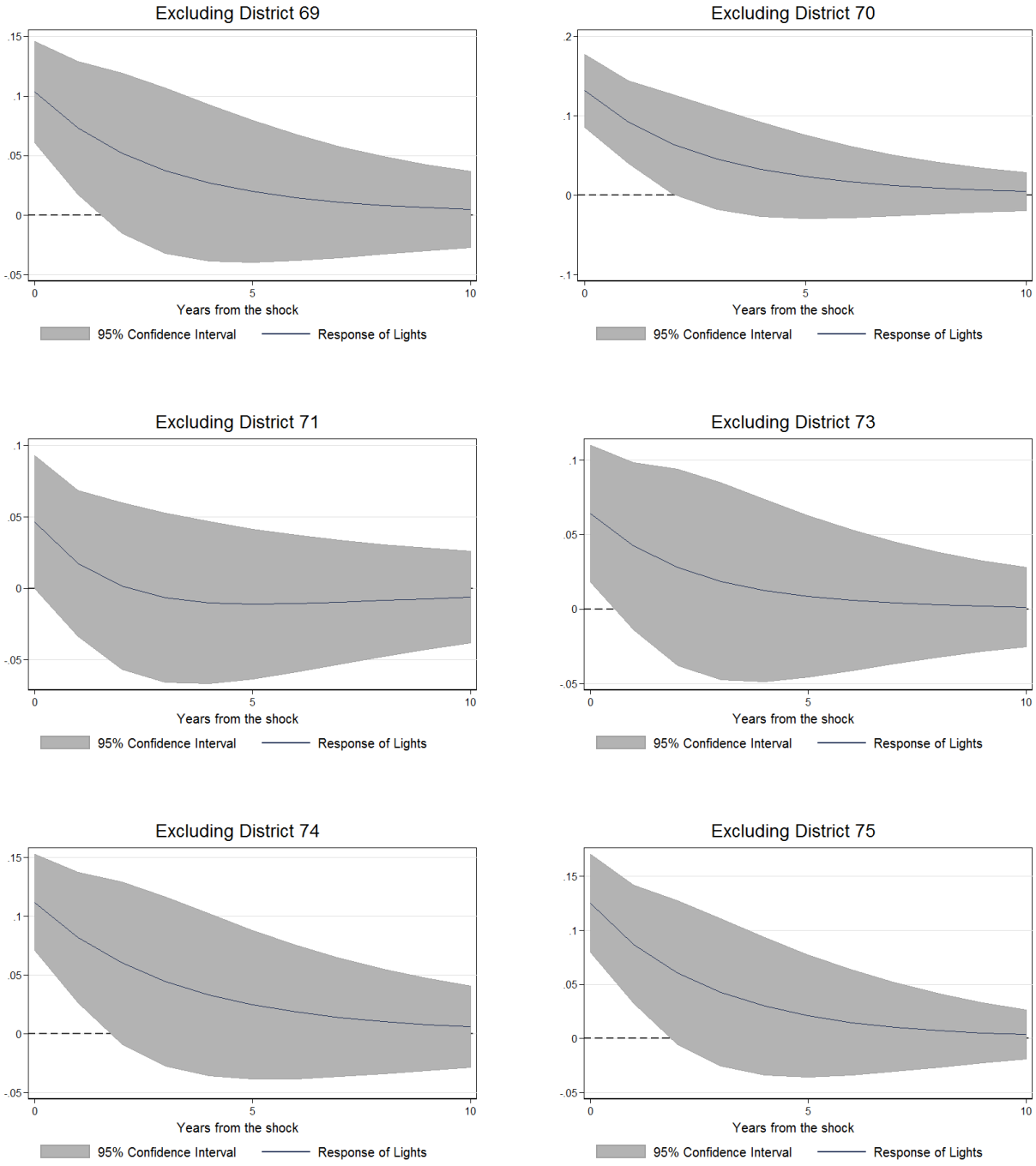

Figure S11: EXCLUDING DISTRICTS 4 – Time-only responses of nightlights to a one standard deviation shock to ODA excluding one district at the time. Years from the shock on the x-axis.

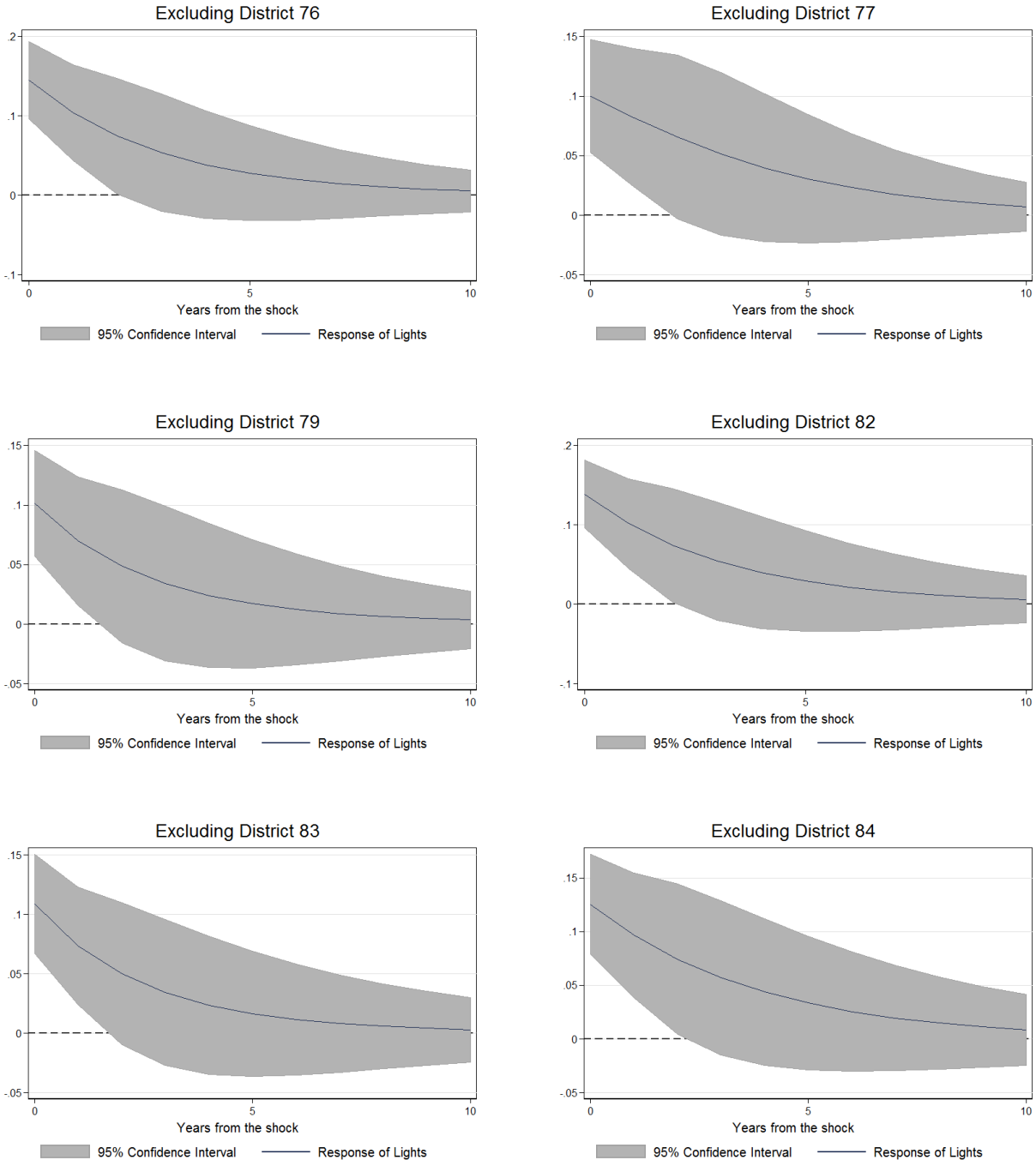

Figure S12: EXCLUDING DISTRICTS 5 – Time-only responses of nightlights to a one standard deviation shock to ODA excluding one district at the time. Years from the shock on the x-axis.

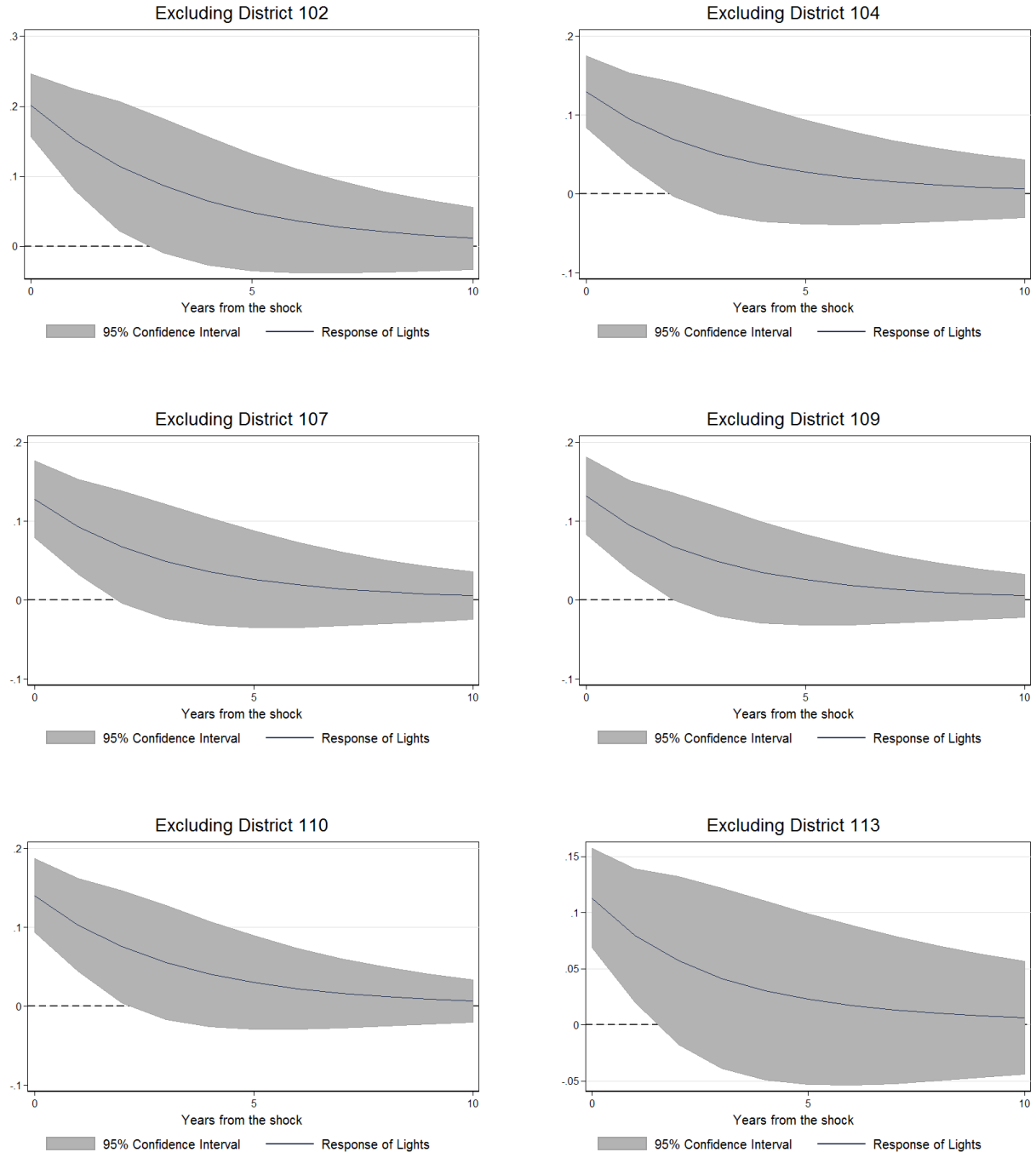

Figure S13: EXCLUDING DISTRICTS 6 – Time-only responses of nightlights to a one standard deviation shock to ODA excluding one district at the time. Years from the shock on the x-axis.

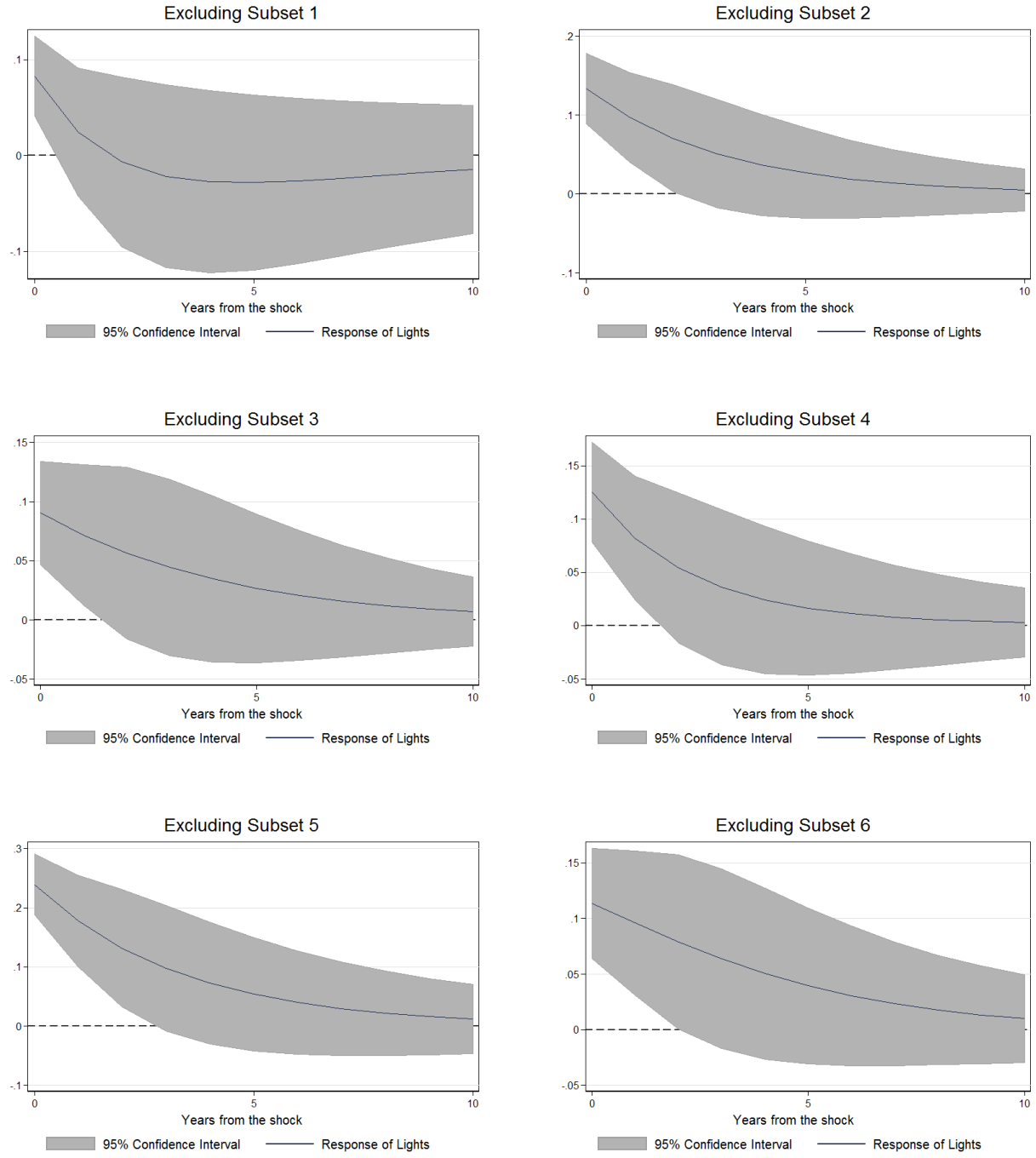

Figure S14: EXCLUDING SUBSET OF DISTRICTS 1 – Time-only responses of nightlights to a one standard deviation shock to ODA excluding a small subset of neighbor districts at the time. Years from the shock on the x-axis.

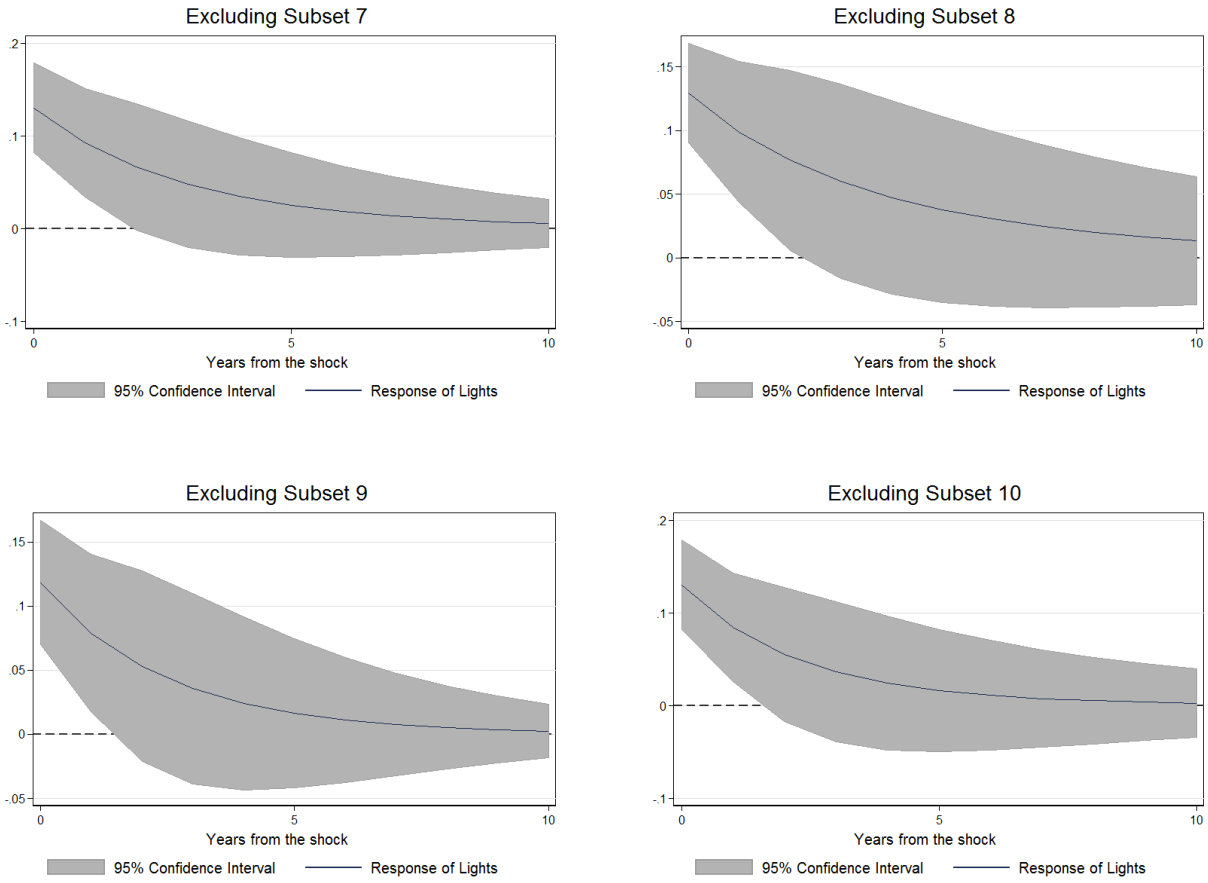

Figure S15: EXCLUDING SUBSET OF DISTRICTS 2 – Time-only responses of nightlights to a one standard deviation shock to ODA excluding a small subset of neighbor districts at the time. Years from the shock on the x-axis.

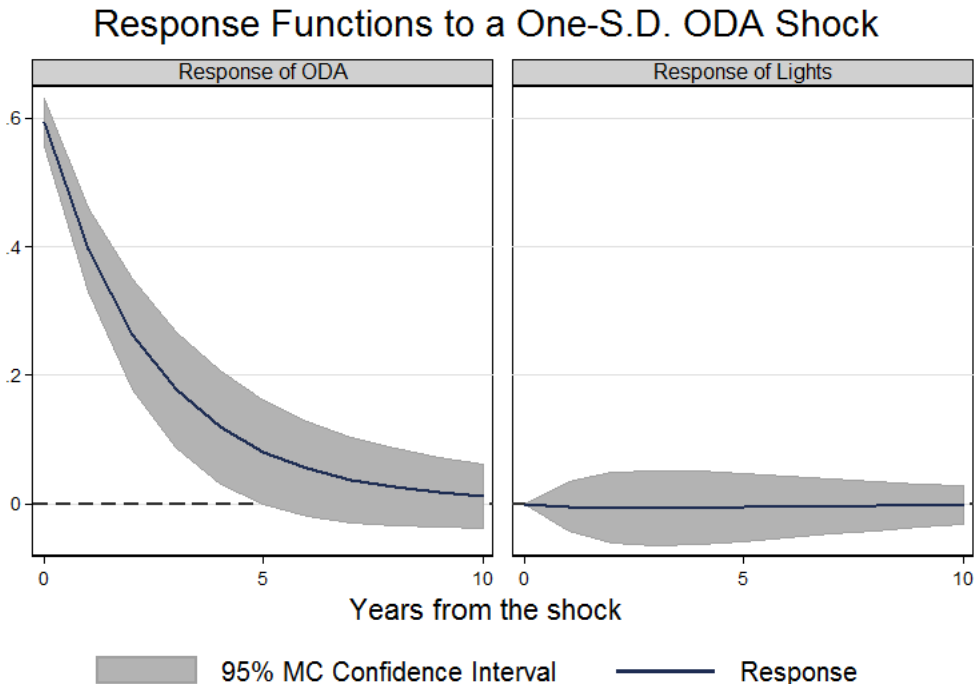

Figure S16: Time-only response functions to a one standard deviation shock to aid disbursements. Identification ordering: oda, light. Years from the shock on the x-axis.

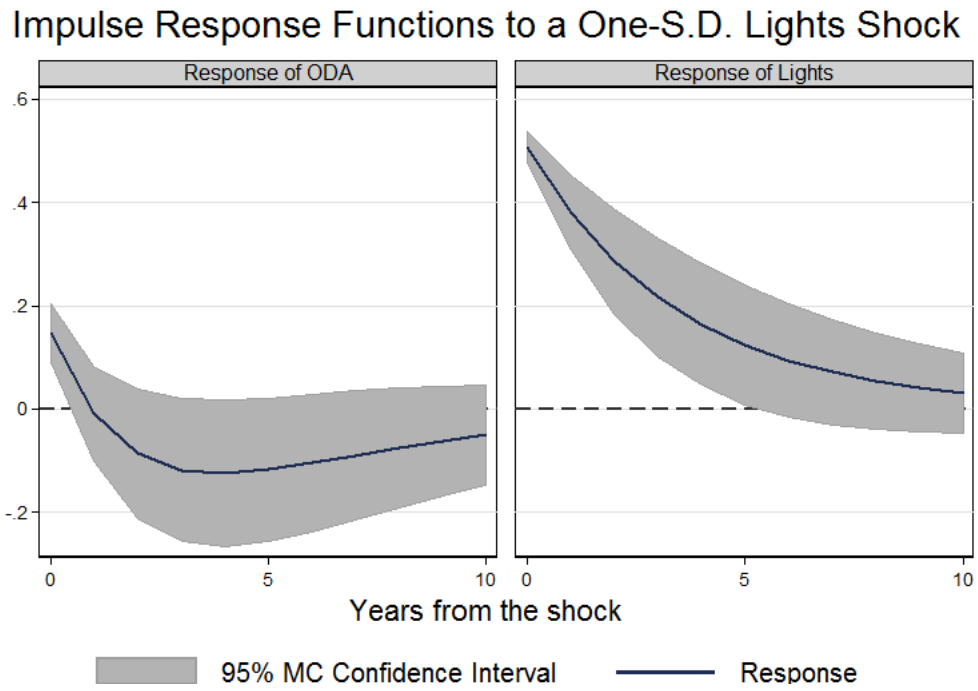

Figure S17: Time-only response functions to a one standard deviation shock to lights. Identification ordering: oda, light. Years from the shock on the x-axis.

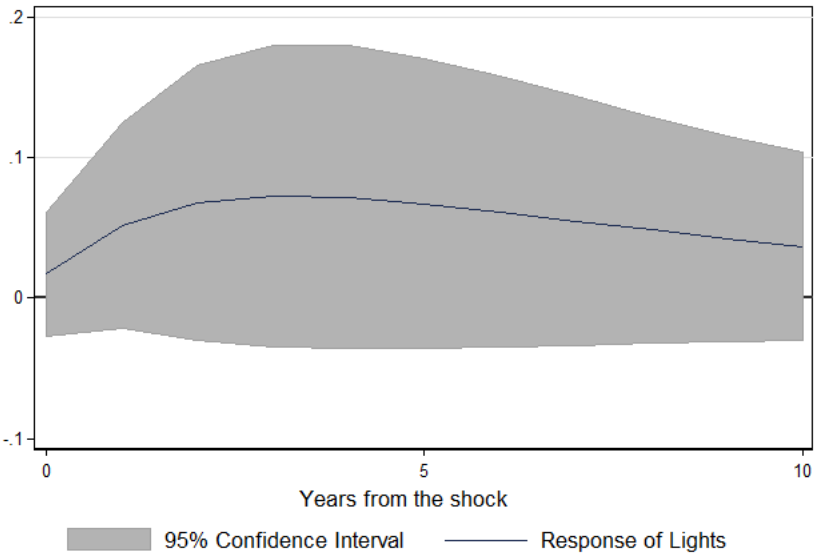

Figure S18: Time-space response of nightlight to a one standard deviation shock to ODA. Only second-lag instrumentation. Identification ordering: oda, light. Years from the shock on the x-axis.

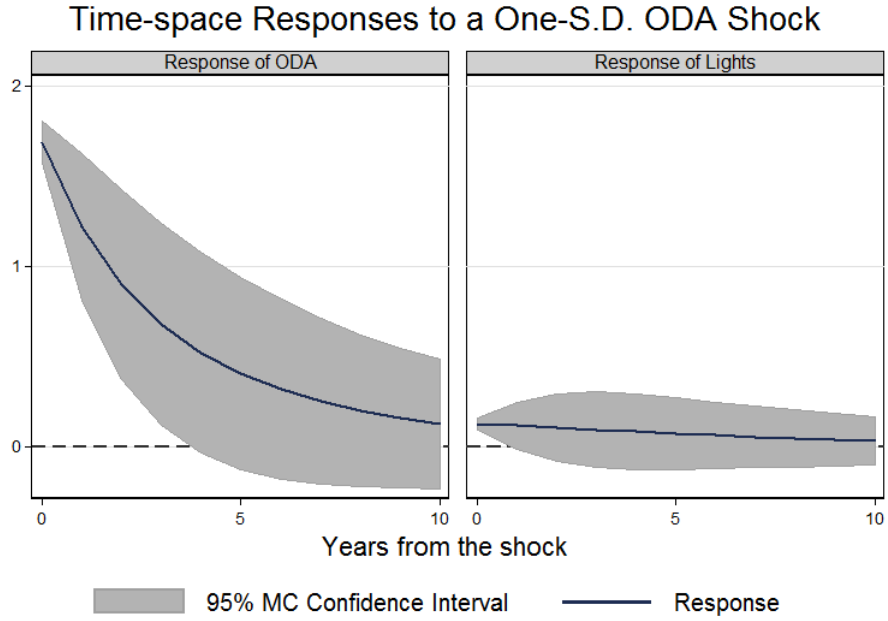

Figure S19: World Bank Dataset: Time-space responses functions to a one standard deviation shock to lights. Identification ordering: oda, light. Years from the shock on the x-axis.

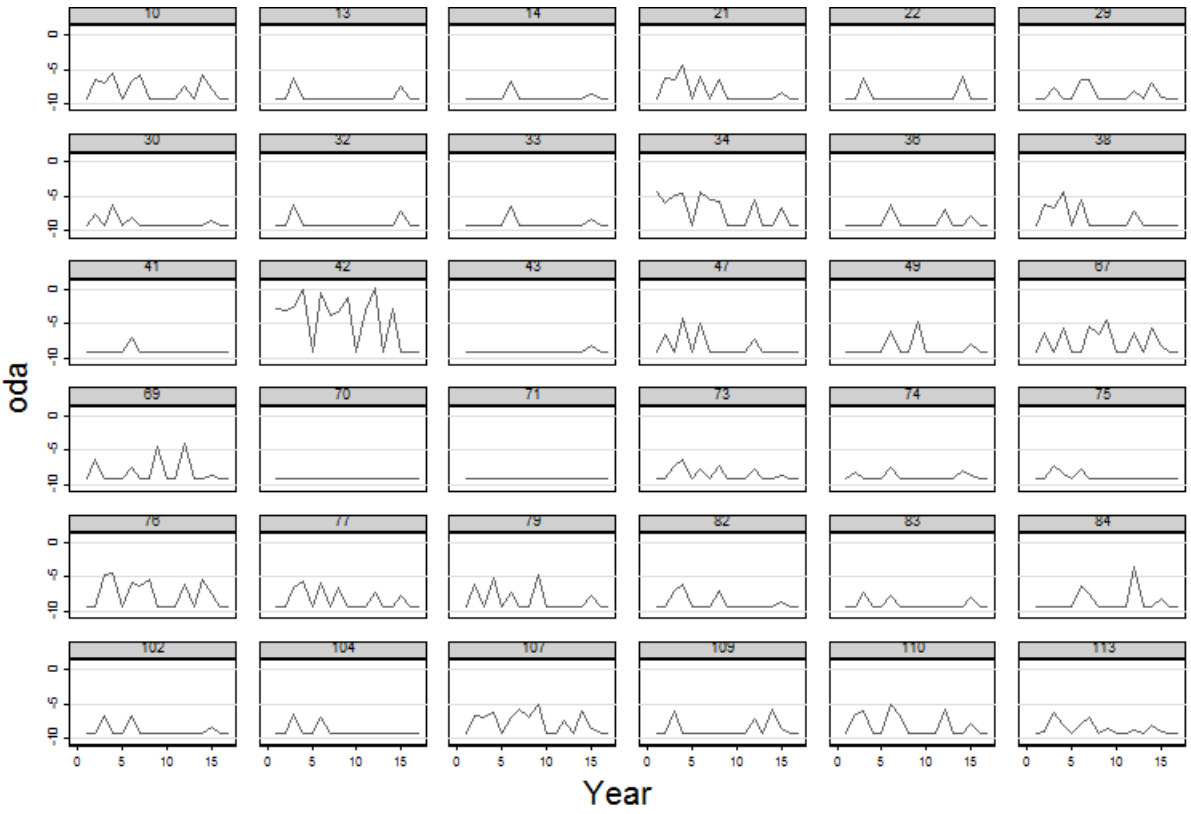

Figure S20: Time series of the variable $oda_{i,t}$ by district for the World Bank dataset.

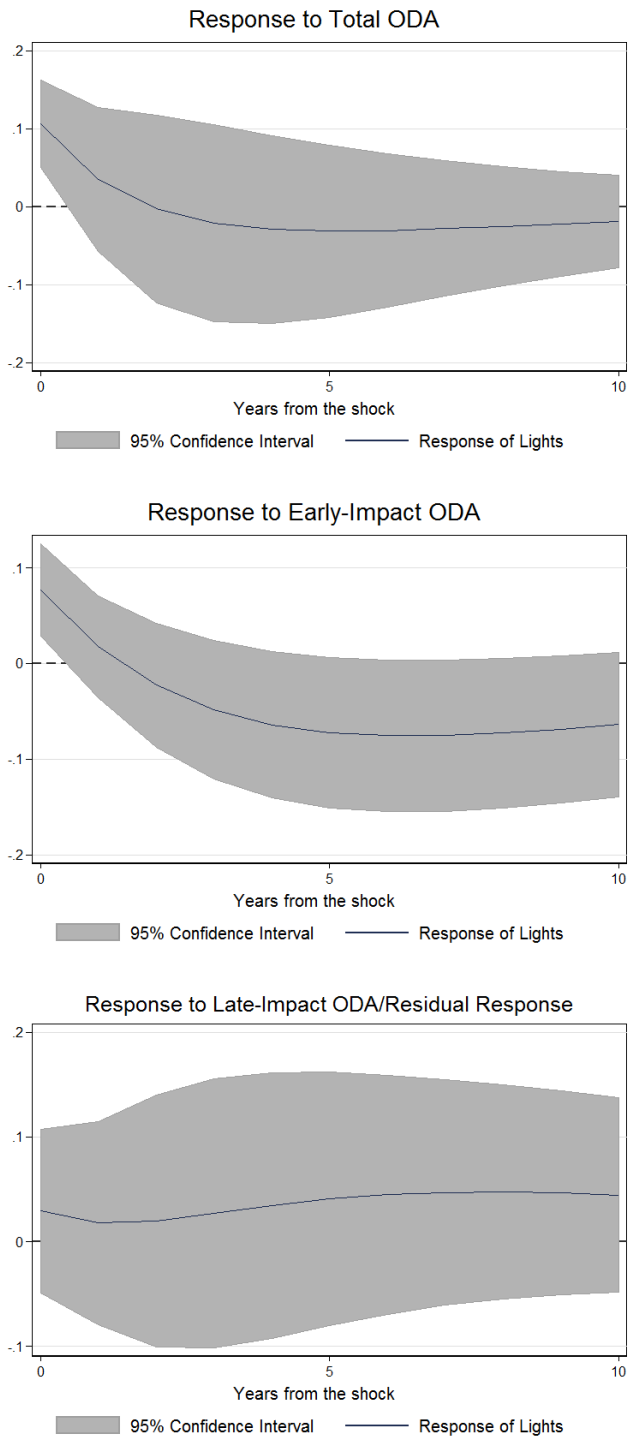

Figure S21: Early-Impact ODA: Time-only responses to a one standard deviation shock to total ODA, early-impact ODA only, and the residual response/late-impact ODA. Identification ordering: oda, light. Years from the shock on the x-axis.

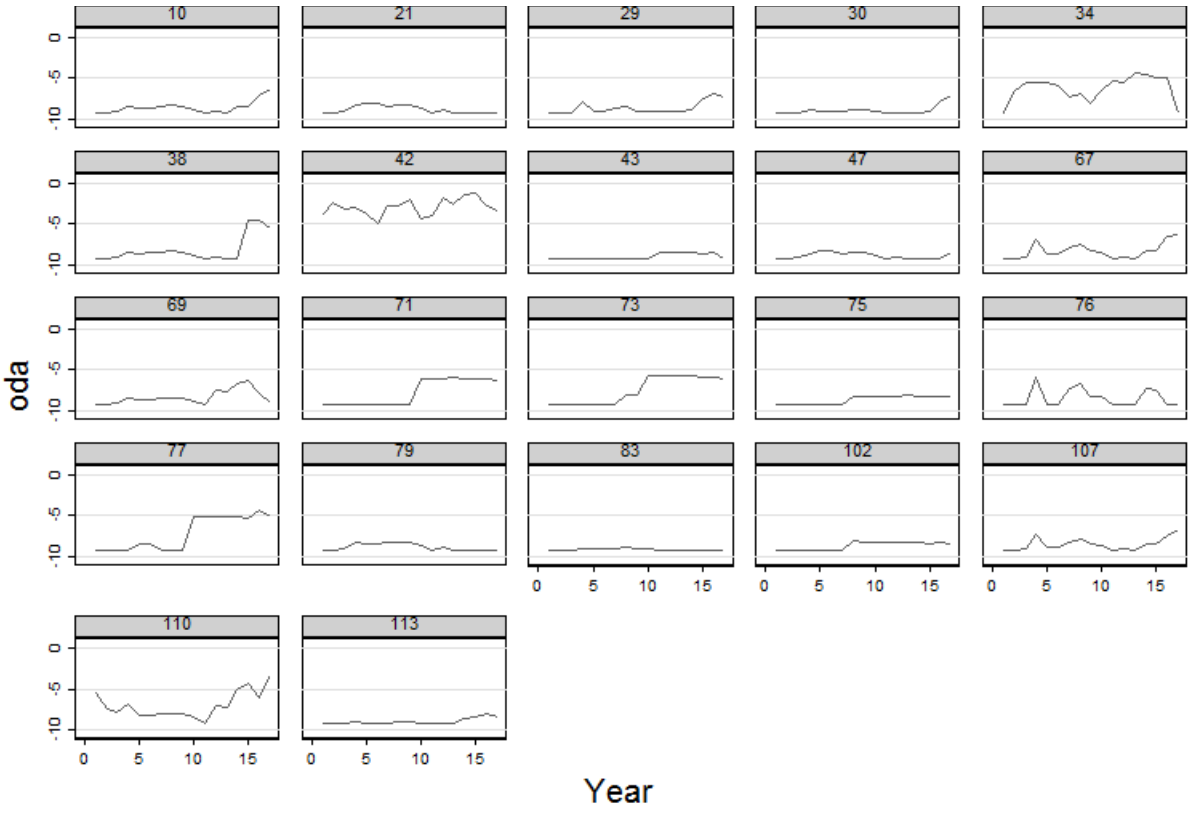

Figure S22: Time series of the variable $oda_{i,t}$ by district for the early-impact ODA dataset.

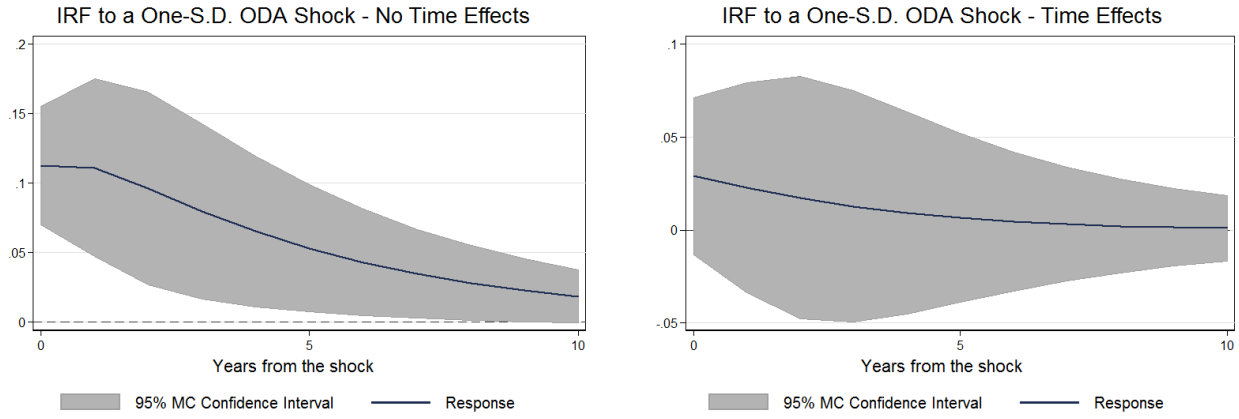

Figure S23: Impulse response of nightlight to a one standard deviation shock to ODA. Basic P-VAR model with no spatial components and baseline specification for GMM estimation. Time effects included in the right panel only. Identification ordering: oda, light. Years from the shock on the x-axis.

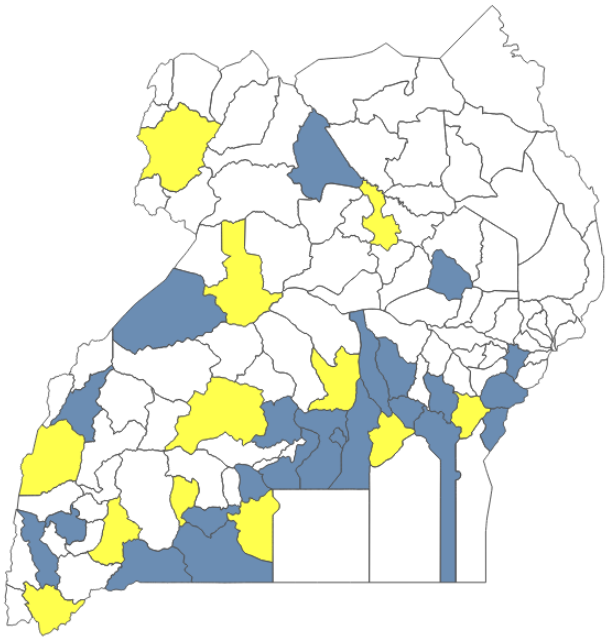

Figure S24: Not-connected districts selected for the aspatial analysis - in yellow.

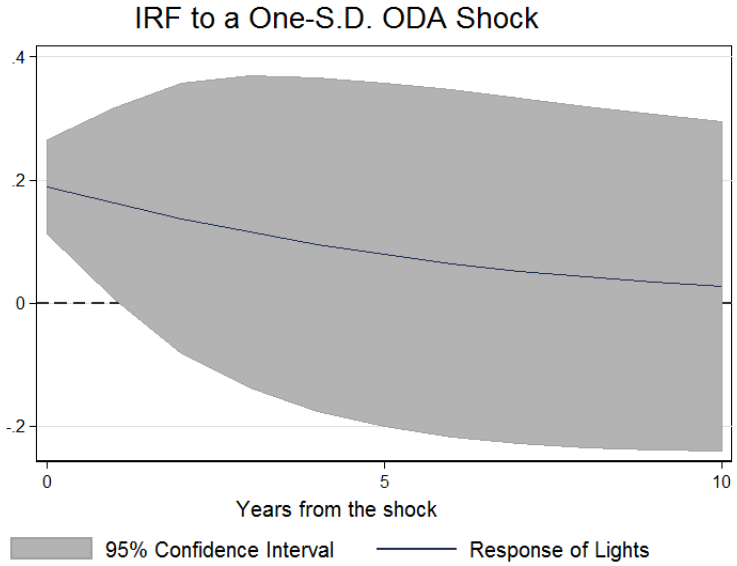

Figure S25: Impulse response of nightlight to a one standard deviation shock to ODA. Basic P-VAR model with no spatial components and weakened neighborhood links for 12 districts that do not share any border. Time effects are included. Identification ordering: oda, light. Years from the shock on the x-axis.

References

Bai, J., and S. Ng (2004): "A PANIC Attack on Unit Roots and Cointegration," *Econometrica*, 72(4), 1127–1177.

Holtz-Eakin, D., W. Newey, and H. S. Rosen (1988): "Estimating Vector Autoregressions with Panel Data," *Econometrica*, 56(6), 1371–1395.

Im, K. S., M. H. Pesaran, and Y. Shin (2003): "Testing for unit roots in heterogeneous panels," *Journal of Econometrics*, 115(1), 53–74.

Pesaran, M. H. (2004): "General Diagnostic Tests for Cross Section Dependence in Panels," CESifo Working Paper Series 1229, CESifo Group Munich.

Reese, S., and J. Westerlund (2016): "Panicca: Panic on Cross-Section Averages," *Journal of Applied Econometrics*, 31(6), 961–981.

Roodman, D. (2009): "How to do xtabond2: An introduction to difference and system GMM in Stata," *Stata Journal*, 9(1), 86–136.

Sarafidis, V., T. Yamagata, and D. Robertson (2009): "A test of cross section dependence for a linear dynamic panel model with regressors," *Journal of Econometrics*, 148(2), 149–161.